Environmental Science & Technology

pubs.acs.org/est

Article

Oxygenated and Nitrated Polycyclic Aromatic Hydrocarbons in Ambient Air—Levels, Phase Partitioning, Mass Size Distributions, and Inhalation Bioaccessibility

Gerhard Lammel,* Zoran Kitanovski, Petr Kukučka, Jiří Novák, Andrea M. Arangio, Garry P. Codling, Alexander Filippi, Jan Hovorka, Jan Kuta, Cecilia Leoni, Petra Příbylová, Roman Prokeš, Ondřej Sáňka, Pourya Shahpoury, Haijie Tong, and Marco Wietzoreck

Cite This: *Environ. Sci. Technol.* 2020, 54, 2615−2625

Read Online

ACCESS | Metrics & More | Article Recommendations | Supporting Information

ABSTRACT: Among the nitrated and oxygenated polycyclic aromatic hydrocarbons (NPAHs and OPAHs) are some of the most hazardous substances to public health, mainly because of their carcinogenicity and oxidative potential. Despite these concerns, the concentrations and fate of NPAHs and OPAHs in the atmospheric environment are largely unknown. Ambient air concentrations of 18 NPAHs, 5 quinones, and 5 other OPAHs were determined at two urban and one regional background sites in central Europe. At one of the urban sites, the total (gas and particulate) concentrations of Σ_{10}OPAHs were 10.0 ± 9.2 ng/m^3 in winter and 3.5 ± 1.6 ng/m^3 in summer. The gradient to the regional background site exceeded 1 order of magnitude. Σ_{18}NPAH concentrations were typically 1 order of magnitude lower than OPAHs. Among OPAHs, 9-fluorenone and (9,10)-anthraquinone were the most abundant species, accompanied by benzanthrone in winter. (9,10)-Anthraquinone represented two-thirds of quinones. We found that a large fraction of the target substance particulate mass was carried by submicrometer particles. The derived inhalation bioaccessibility in the PM_{10} size fraction is found to be ≈5% of the total ambient concentration of OPAHs and up to ≈2% for NPAHs. For 9-fluorenone and (9,10)-anthraquinone, up to 86 and 18%, respectively, were found at the rural site. Our results indicate that water solubility could function as a limiting factor for bioaccessibility of inhaled particulate NPAHs and OPAHs, without considerable effect of surfactant lipids and proteins in the lung lining fluid.

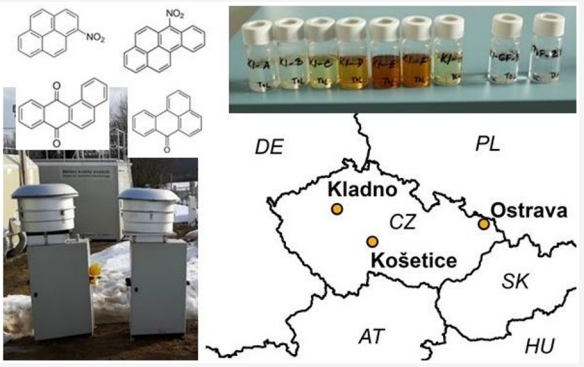

1. INTRODUCTION

Organic chemicals contribute significantly to air pollution and its adverse health effects.[1,2] A number of parent polycyclic aromatic hydrocarbons (PAHs), including the often monitored benzo[*a*]pyrene have been identified as substances of high concern;[3] some are mutagenic and carcinogenic[4] and across Europe PAHs represent the greatest environmental exposure health risk.[5] Many organic contaminants in the atmosphere are bound to fine particles. The health risk attributable to more polar constituents of particulate organic matter (POM) is not fully characterized and it is potentially related to diseases most commonly attributed to cigarette smoke exposure.[1,6,7] This fraction contains the strongest mutagens, which are nitrated PAHs (NPAHs, such as the dinitropyrenes), and the quinones, a subgroup of oxygenated PAHs (OPAHs). The mutagenicity and carcinogenicity of many quinones is high compared to parent PAHs,[8] because they form strong DNA adducts.[9] Moreover, quinones, through redox cycling with the corresponding semi- or hydro-quinones, promote formation of reactive oxygen species (ROS) and some of them are strong mutagens and carcinogens. ROS cause oxidative stress associated with chronic diseases.[10,11] The NPAHs' biological effects are usually stronger than those of the parent compounds (PAHs). This has been documented for the mutagenicity of fluoranthene, pyrene, chrysene, and benzanthrone (BAN) and their nitrated derivatives[8,12−15] and for developmental toxicity of phenanthrene, anthracene, pyrene, and BAN and their nitrated derivatives.[16]

NPAHs and OPAHs are co-emitted with soot in all combustion processes and they are abundant in polluted air.[17−19] Several (or many) NPAHs and OPAHs are formed through photoreactions of PAHs.[20,21]

Received: November 13, 2019
Revised: January 7, 2020
Accepted: January 17, 2020
Published: January 17, 2020

https://dx.doi.org/10.1021/acs.est.9b06820
Environ. Sci. Technol. 2020, 54, 2615−2625

Whereas PAHs are regularly monitored and have been extensively studied in the atmospheric environment, NPAH and OPAH are not included in existing air monitoring programs, and have only recently attracted attention in the context of urban air quality. In urban areas, the concentrations of ΣNPAHs and ΣOPAHs are typically in the of range 0.1−3 and 4−20 ng m^{-3}, respectively,[22−26] though the number of compounds included in each study differs, leading to additional variance. Little is known about the NPAHs' and OPAHs' atmospheric fate and distribution in background atmospheres and remote environments compared to urban areas.[22,23,25,27−31] OPAHs in air have been only occasionally studied in rural or remote environments.[17,22]

Heterogeneous oxidation of PAHs and quinones and incomplete combustion processes lead to the formation of environmentally persistent free radicals (EPFRs) included in particulate matter (PM[32]). EPFRs are organic radicals with semiquinone-like and phenoxyl-like chemical structure having lifetimes of > 1 day (up to months). Semiquinones are intermediates in quinone/hydroquinone chemistry.[33] Also, nitration may turn parent PAHs into a ROS-generating compound.[34−37] Upon dissolution in water, EPFRs are able to form ROS through a catalytic process. . Therefore, EPFRs play a key role in the oxidation process and redox chemistry of PAH, and in generating ROS.[38,39]

However, the complete pollutant mass in air may not be bioaccessible upon inhalation as dissolution of the substance in the epithelial lung lining fluid (LLF) is a prerequisite for biological activity. This prerequisite is not needed, however, when the substances are carried by ultrafine particles, which may penetrate membranes completely.[40,41] Unlike heavy metals in PM,[42,43] the fraction of POM that is soluble in LLF has hardly been studied.[44]

The aim of this present study was to determine concentrations of NPAHs and OPAHs in the aerosol in central Europe, spanning the range from background air to heavily polluted air. The long-range transport potential of these pollutants is addressed by determining the particulate mass fraction and the mass size distribution. Furthermore, we study the concentration of EPFR in the samples. For the first time, we quantify inhalation bioaccessibility of these pollutants in particulate matter (PM) based on solubility in simulated LLF. The biological effects of the targeted compounds are the focus of a companion paper.[45]

2. MATERIALS AND METHODS

2.1. Sampling Sites. Air samples were collected at two urban and one rural site in the Czech Republic, Kladno-Švermov (50°10′01″N/14°06′15″E) during 10−14 February 2016, Ostrava-Přivoz (49°51′23″N/18°16′11″E) during 15−27 February and 5−17 September 2016 and Košetice (49°34′24″N/15°04′49″E) during 13 February to 3 March 2017, respectively (Figure S1). In Kladno, an industrial town (≈70,000 inhabitants), no major industries were working during the campaign. The Ostrava site is located relatively central to the industrial area (≈500,000 inhabitants). It is a station of the Czech Hydrometeorological Institute (CHMI), and within 3 km of the site are 210 coke (fuel coke) furnaces, a large metallurgical plant, a waste incinerator, and other industries. Ostrava is a hot spot of air pollution in Europe.[46−48] Previous studies have measured parent PAH abundance to be significantly greater than reference sites and the biological effects of PM are evident, especially during winter.[49−52]

The rural site, Košetice, is in the central Czech Republic located in a mixed agricultural and forested area. This site reflects the central European background and is part of the European Monitoring Environmental Programme (EMEP).

2.2. Sampling. Particulate and gas phase samples were collected side by side by a high-volume air sampler Digitel DH77 (DIGITEL, Hegnau, Switzerland) and a high-volume six-stage slot impactor Baghirra HV-100P (Baghirra, Prague, CZ). All samplers had PM_{10} inlets. The DIGITEL sampler was equipped with a quartz fiber filter (QFF, Whatman GE, Buckinghamshire, UK) and, downstream, two polyurethane foam (PUF) plugs (Molitan, Břeclav, Czech Republic, density 0.030 g cm^{-3}, placed in a glass cartridge) in series (0.95 L total volume). The Baghirra sampler was equipped with a multistage cascade impactor (Tisch Environmetal Inc., Cleves, USA, series 230, model 235) with five impactor stages, corresponding to 10−7.2, 7.2−3, 3−1.5, 1.5−0.95, and 0.95−0.49 μm of aerodynamic particle size, D, (spaced roughly equal $\Delta \log D$) and a backup filter collecting particles <0.49 μm. In the impactor, PM was collected on a slotted QFF (TE-230-QZ, Tisch Environmental Inc., Cleves, USA, 14.3 × 13.7 cm) and the backup filter was a QFF (Whatman). PUFs were cleaned [8 h-extraction in acetone and 8 h in dichloromethane (DCM)], wrapped in two layers of aluminum foil, placed into zip-lock polyethylene bags, and kept in the freezer prior to deployment. The samplers were operated at constant flow rates of ≈29 (Digitel, 24 h sampling) and ≈68 m^3 h^{-1} (Baghirra, 96 h sampling).

During each sampling campaign, the deployed filter and PUF samples were kept on site and during transport remained in cool boxes at ≈0 °C, then stored at ≤−18 °C until gravimetry, cutting (and punching) and subsequent extraction (or LLF leaching). For ESR, the filter punches were kept at ≈−78 °C.

2.3. Chemical Analysis. Air samples, PUFs, and QFFs, were extracted using automated warm Soxhlet extraction. The NPAHs and OPAHs were analyzed by atmospheric pressure gas-chromatography tandem mass spectrometry (GC-APCI-MS/MS). Details and QA data are given in the Supporting Information, S1.2.

Ten OPAHs were targeted (Σ_{10}OPAHs), that is, 1,4-naphthoquinone ((1,4)O_2NAP), 1-naphthylaldehyde (1-(CHO)NAP), 9*H*-fluoren-9-one (9OFLN), 1,4- and 9,10-anthraquinone ((1,4)-, (9,10)O_2ANT), 11*H*-benzo[*a*]- and -[*b*]fluoren-11-one (11OBaFL, 11OBbFL), BAN (or 7*H*-benzo[*de*]anthracene-7-one), benzo[*a*]anthracene-7,12-dione ((7,12)O_2BAA) and 5,12-naphthacenequinone ((5,12)-O_2NAC, also called tetracenequinone). 18 NPAHs were targeted (Σ_{18}NPAHs), namely, 1- and 2-nitronaphthalin (1-, 2NNAP), 3- and 5-nitroacenaphthene (3-, 5NACE), 2-nitrofluorene (2NFLN), 9-nitroanthracene (9NANT), 3- and 9-nitrophenanthrene (3-, 9NPHE), 2- and 3-nitrofluoranthene (2-, 3NFLT), 1- and 2-nitropyrene (1-, 2NPYR), 7-nitrobenzo[*a*]anthracene (7NBAA), 6-nitrochrysene (6NCHR), 1,3-, 1,6- and 1,8-dinitropyrenes ((1,3)-, (1,6)-, (1,8)N_2PYR) and 6-nitrobenzo[*a*]pyrene. All concentration data are corrected for field blank levels. The method and QA/QC are described in detail in Supporting Information, S1.2. The acronyms and chemical structures of the targeted compounds are shown in Table S1a,b of the Supporting Information.

EPFRs in the lowermost impactor stage samples (<0.49 μm) were analyzed using continuous-wave electron paramagnetic

https://dx.doi.org/10.1021/acs.est.9b06820
Environ. Sci. Technol. 2020, 54, 2615−2625

Table 1. Overview of Pollution during Campaigns: Targeted Organic Pollutant Concentrations (OPAH, NPAH) Total ($c_{total} = c_g + c_p$) Concentrations (ng m^{-3}; Mean (min−max) (Mixing Ratios in PM_{10}, ppmm), Together with PM Size Fraction Concentrations PM_{10}, $PM_{2.5}$ ($\mu g\ m^{-3}$) Inorganic Gaseous Pollutants and Meteorological Data[a]

	rural background	urban		
	Košetice winter	Kladno winter	Ostrava winter	Ostrava summer
Σ_{10}OPAH (ng m^{-3})	0.51 (0.26−0.83)	5.6 (2.2−9.0)	10.0 (2.3−34.2)	3.98 (0.59−6.56)
Σ_{10}OPAH (ppmm)	(44)	(380)	(250)	(99)
Σ_{18}NPAH (ng m^{-3})	0.016 (0.004−0.037)	0.064 (0.004−0.14)	1.8 (0.2−8.1)	1.05 (0.09−2.28)
Σ_{18}NPAH (ppmm)	(1.2)	(3.3)	(45)	(26)
$PM_{10}/PM_{2.5}$ ($\mu g\ m^{-3}$)	9.1/5.9	16.9/15.4	39.9/34.2	40.2/30.1
EC/OC ($\mu g\ m^{-3}$)	0.1/1.4	0.9/6.9	1.4/7.1	1.4/6.0
NO_x/CO (ppbv)	6.5/217	15.4/320	45.1/496	41.3/375
$SO_4^{2-}/NO_3^-/NH_4^+$ ($\mu g\ m^{-3}$)	1.1/2.3/1.8	1.1/3.9/1.8	2.2/4.2/3.2	n.d.
Fe/Pb (ng m^{-3})	62/1.2	186/6.8	977/21	1285/20
temperature (°C)	4.9 (−2 to −13)	0.9 (−6 to −10)	4.1 (−4 to −15)	20 (11−29)
rel. humidity (%)	72 (35−98)	79 (47−95)	80 (41−97)	70 (35−95)
wind velocity (m s^{-1})	4.5 (0.6−11.1)	1.4 (<0.2−7.7)	1.2 (<0.1 to −4.0)	0.7 (0.1−2.7)

[a]n.d. = no data.

resonance (EPR) spectroscopy as described in our recent studies.[53,54] The method is described in Supporting Information, S1.3. Meteorological parameters, inorganic trace gases, and aerosol parameters (number concentration) were measured on site. Transition metals, lead, and PM total elemental and carbon fraction concentrations were determined off-line from punches of baked quartz filters. The methods are described in the Supporting Information, S1.5.

2.4. Bioaccessibility. For the bioaccessible fractions of the target substances in PM, f_{bio}, 1.2 cm^2 of QFFs were immersed in 20 mL of simulated LLF by shaking (60 rpm) in a 100 mL flask for over 24 h in an incubator at 37 °C, in the dark. For QFFs exposed below impactor slots, each three out of the 10 strips (length 12 cm) were leached. The leachates were filtered (0.45 μm cellulose acetate membrane), spiked with internal standards, concentrated, and purified on SPE disks [BAKERBOND Speedisk DVB H_2O-philic, sequentially methanol and methanol/acetone (1:1) elution]. Two simulated LLFs were used, that is,, either artificial lysosomal fluid (ALF[55]) or modified Gamble's solution (SELF[56]). ALF mimics the chemical environment created by macrophage activity. It is an acidic aqueous electrolyte without lipids, pH 4.5. SELF mimics both viscous and lipid qualities. It is a dispersion of a neutral aqueous electrolyte with lipids, proteins, and antioxidants, pH 7.4. The compositions are given in the Supporting Information, Table S2.

The NPAH and OPAH concentrations in LLF leachates were obtained by liquid−liquid extraction using 5 mL of *n*-hexane/DCM (4:1) mixture for 5 min, in an orbital shaker. The extraction was repeated three times and extracts pooled for further clean-up. The extract was cleaned using a silica column (5 g of silica, 0.063−0.200 mm, activated at 150 °C for 12 h, 10% deactivated with water) and 1 g of Na_2SO_4. Target compounds were eluted with 5 mL of *n*-hexane followed by 50 mL of DCM. The eluate volume was reduced by a stream of nitrogen in a TurboVap II (Caliper Life Sciences, USA) concentrator unit and transferred into a vial. Terphenyl and PCB121 were added as internal injection standards; the final volume was 200 μL. NPAHs and OPAHs were determined using the same method as for DCM extracts; see Section 2.3.

The bioaccessible fraction was derived as $f_{bio\_p} = c_{p\ LLF}/c_{p\ DCM}$. Larger uncertainties propagated for low concentrations $c_{p\ LLF}$ and $c_{p\ DCM}$ [close to limit of quantification (LOQ)] whenever blank values varied considerably. This applied to 1(CHO)NAP in the Košetice and for (1,4)O_2NAP in the Ostrava winter campaign.

3. RESULTS AND DISCUSSION

3.1. Concentration Levels, Phase, and Mass Size Distributions. The levels of the targeted substance classes in air (total concentrations, i.e., gas and particulate) during the campaigns are listed in Table 1 and the time series are shown in Figure S2. The urban sites are noticeably more polluted than the rural background site. This applies not only to OPAHs, which are completely or mostly from primary emissions, but also to NPAHs, which to a large extent are formed through photoreactions of PAH (secondary sources).[20,21] The urban−rural contrast is also reflected in the PM_{10} and $PM_{2.5}$ concentrations, the C, Fe, and Pb contents of PM, and the NO_x and CO levels (Table 1; additional elements in PM are presented in Figure S3). Nevertheless, the levels at the background site, Košetice, clearly indicate polluted air, which was also noted by previous studies.[57−59] The OPAH concentrations at the Košetice and Ostrava sites corresponded to 5−10% of the parent PAH levels typically observed there in these seasons.[59−62] NPAHs corresponded to 20−25% of OPAHs at the urban site Ostrava, in both seasons, but to only ≈3 and ≈1% of OPAHs at the rural background and the urban site Kladno, respectively (Table 1). In PM_{10}, the mass mixing ratio of OPAHs was 250 ppmm (0.025%) and of NPAHs 45 ppmm in Ostrava in winter; ≈50% of these values were found at the same site in summer and ≈20% of these at the background site in winter (Table 1).

The pollution by heavy metals in Ostrava air were found particularly high, and independent of season (Table 1, Figure S3), and must be seen in the context of the local metallurgical industries and coal production and burning.[46,61] For example, Fe and Zn at our urban site in Ostrava fall within the ranges spanned by other sites in Ostrava[61] and exceed typical levels of urban areas in Europe (e.g., by a factor of 3 for Grenoble, France[63]). The pollution at the urban sites is less reflected by the levels of the secondary inorganic aerosol (SO_4^{2-}, NO_3^-, NH_4^+), because these are regionally distributed pollutants, exhibiting a low urban-to-rural gradient.[64]

The particulate mass fractions, $\theta = c_p/(c_g + c_p)$, varied considerably across sites and seasons (Table S3): the shift to

https://dx.doi.org/10.1021/acs.est.9b06820
Environ. Sci. Technol. 2020, 54, 2615−2625

the gas-phase from winter to summer is very pronounced for the NPAHs, found almost completely in the gas-phase in the Ostrava summer campaign. This behavior resembles that of parent PAHs, which is caused by the effect of temperature on the interaction energies of the PM adsorbing and absorbing phases.[31,65] The phase partitioning is somewhat inconsistent for OPAHs, with θ higher for (1,4)O_2NAP, 1(CHO)NAP and 9OFLN in summer, and also for Σ_{10}OPAH (θ = 0.88 vs 0.77 in winter; Table S3b). (1,4)O_2NAP and 9OFLN are expected to be mainly in the gas-phase in winter, with estimated $\theta \leq 0.2$ at freezing point;[66] lower θ is expected for these substances in summer. Low particulate mass fraction in winter could be explained by slow relaxation to equilibrium in the immediate vicinity of the source, which may become significant if the emission temperature is far higher than the ambient temperature. In fact, during the summer days with maximum values of the aforementioned OPAHs, advection was from northerly directions, which was rare during the winter campaign. These high OPAH levels could be related to emission sources in this highly industrial area, north of the site. Wind velocity was very low during all campaigns at the urban sites, whereas it was elevated at the background site. Correspondingly, mixing was certainly lower at the urban sites (located in the low land) than at the background site (highland).

The OPAH levels at Ostrava reflect the site as a hot spot of air pollution. Most OPAH levels indicate that contamination is greater in comparison with other urban sites worldwide.[17] However, the PAH concentrations reported in polluted areas of North China and North India were even higher (e.g., refs 67 and 68). The levels at the other urban site, Kladno, were approximately half those in Ostrava, and an order of magnitude higher than at the background site, Košetice (Table 1).

The NPAH levels varied much more across sites, in the range of 0.01−10 ng m^{-3}, which is the NPAH concentration range anticipated for polluted atmospheres in general.[18,19] Noticeable is the big difference of NPAH levels at the two urban sites, much greater than for OPAHs, which indicates strong local sources of NPAH at Ostrava (Table 1). This is most likely related to domestic heating, as these sources are insignificant in summer. Fuel use in the two areas, however, is reported to be rather similar.[69] It should be noted that higher atmospheric mixing typically occurring during summer did not contribute to the seasonal gradients in Ostrava, as indicated by the same PM_{10} and $PM_{2.5}$ levels during the winter and summer campaigns (Table 1). Half of this NPAH gradient is actually explained by one substance, 9NANT (0.85 and 0.01 ng m^{-3} in winter and summer, respectively; Table S3a, Figure S4a). The relatively high abundance of 9NANT in the particulate phase in both precipitation and air was previously reported from urban and background sites in the region.[66,70] Similar gradients between the urban sites (and insignificance in Ostrava in summer) are found for the four-ring OPAHs (11OBaFL through (5,12)O_2NAC; Table S3b). 9NANT is a major component of PAH and its derivatives' exposure in households using coal, but also wood[71,72] and was found in ambient air dominated by road traffic emissions (diesel[20]). High OPAH concentrations observed in Ostrava in winter may be strongly influenced by major polluters in the urban area, that is, a coke plant (≈1 km away), a metallurgical plant (ca. 3 km away, with a coke oven, sintering plant, and blast furnace), and coal combustion in general.[73] Coal burning for domestic heating is another significant source during the cold season. A small fraction, ≈2.5%, of the households in the Ostrava area use coal exclusively for heating and up to 20% of households may use coal occasionally; both fractions are similar to the average use in the Czech Republic.[69] The strong fingerprint of coal on PAHs in air has been verified in winter atmospheric monitoring previously.[74] A significantly greater number of households in neighboring Poland may use coal[75] and could influence winter concentrations. Because of high coal usage and low energy efficiency, Polish cities rank highest on air pollution indicators in Europe.[76]

Most of the NPAH and OPAH in the particulate phase were carried by submicrometer particles, that is, 55−95% (campaign means, Table S4a, Figures S5 and S7). This corresponded to mass median diameters (MMDs) in the range 0.08−0.14 and 0.06−0.82 μm for NPAHs and OPAHs, respectively (Table S4a).

In most cases, the distribution among the two submicrometer impactor stages was such that more mass was collected on the lowermost stage, that is, $PM_{0.49}$ (Figure S5). However, $PM_{0.49-f0.95}$ exceeded $PM_{0.49}$ for OPAHs in Kladno by far, unlike at other sites (Figure S5). This could be due to the local mix of primary sources. The NPAH and OPAH coarse mass fraction corresponds to <15%. In winter it is highest for OPAHs (and also for the subclass quinones, i.e., O_2PAHs), in summer higher for NPAHs. The PM_1 fraction of OPAHs is even higher in summer, whereas the opposite is found for NPAHs. This shift is in agreement with re-distribution of condensable NPAH in the aerosol. It should be noted that most of NPAHs are gaseous in summer, but associated with the particulate phase in winter (Table S3a). Thus, the redistribution of NPAHs to the larger particle sizes is limited in winter and preferred in summer, although c_p is smaller in summer than in winter. For comparison with the target analytes' mean square displacements (MSDs), the MSDs of PM and of the mineral component (indicated by the iron content), which both showed a supermicrometer maximum, are shown in Figures S5 and S6.

Whereas a maximum of the MSD in the size range 0.1−0.4 μm was reported for OPAHs and NPAHs across all types of sites studied, there is an inconsistency in previous studies such that uni- as well as bimodal MSDs of NPAH and OPAH had been reported.[77−79] Two modes in the range < 0.65 μm have even been reported for some NPAHs, that is, 3NFLT, 3NPHE, and 1NPYR.[80] Note that the low size resolution achieved here (6 stages within PM_{10}) may hide modes, which in particular applies for the so-called accumulation mode, which adds mostly to $PM_{0.49}$, but also to the size fraction between 0.49 and 0.95 μm.

3.2. Substance Patterns. NPAH patterns are dissimilar across seasons, reflecting the significance of secondary sources. Accordingly, only Ostrava winter and the rural background site (winter) are significantly similar (R = 0.69, P < 0.01; Figure S4a). The NPAH pattern observed in Ostrava in summer is very similar (R = 0.92, P < 0.01) to the pattern observed in the Gt. Hungarian Plain in the same season (some 350 km South−Southeast),[31] and even has similarities to the pattern observed over the summer South Atlantic (own unpublished data). This points to the significance (relative abundance) of long-lived (and long-range transported) substances among the targeted NPAHs. The most abundant NPAHs were 2NFLT and 9NANT in winter and the NNAPs in summer. This may point to photolysis limiting the lifetimes of 2NFLT and 9NANT more than other NPAHs. The same seasonal patterns were reported from an urban site in Western Europe (Grenoble,

https://dx.doi.org/10.1021/acs.est.9b06820
Environ. Sci. Technol. 2020, 54, 2615−2625

Table 2. Concentrations of Spin, Water-Soluble Transition Metals (Fe and Cu), OPAHs (Σ_{10}OPAH), and Quinones (Σ_6O_2PAH) in $PM_{0.49}$ [Campaign Mean (min−max)]

	rural background	urban		
	Košetice winter	Kladno winter	Ostrava winter	Ostrava summer
EPFR (pmol μg^{-1})	2.2 (1.3−4.0)	0.8	2.8 (2.1−3.1)	3.1 (2.6−3.9)
EPFR (pmol m^{-3})	1.1 (0.6−1.8)	6.6	24.5 (11.1−40.7)	5.9 (3.8−8.1)
Fe (pmol m^{-3})	158 (<72 to 430)	1400	11,600 (2360−28,000)	3780 (2430−5340)
Cu (pmol m^{-3})	25 (<72 to 102)	<30	85 (47−156)	63 (41−96)
Σ_6O_2PAHs (pmol m^{-3})	0.65 (0.23−1.2)	0.15	4.8 (1.8−8.0)	5.9 (<0.02 to 12)
Σ_{10}OPAHs (pmol m^{-3})	0.91 (0.39−1.6)	0.19	14.1 (4.7−23)	9.1 (<0.03 to 19)

France[24]). The NPAH pattern observed in winter is also similar to the one observed at another central European site in winter, Mainz, Germany (R = 0.84−0.89, P < 0.01[70]) and reflected in snow across sites in the region.[66] Whereas 2NFLT is formed in air, initiated by reaction of FLT with •OH radicals, NNAPs and 9NANT have mostly primary sources (as mentioned above[20,21]). The NPYRs, primary emitted 1NPYR and secondarily formed 2NPYR, were not very abundant unlike found in other studies, where their ratio was reported to vary according to proximity to traffic sources.[79,81] Among the highly carcinogenic N_2PYRs, only (1,6)N_2PYR was found at the urban sites in winter.

Some of the OPAH patterns are significantly similar across sites (R = 0.60−0.75; P < 0.05), others are not (R = 0.45−0.50; Figure S4b). Most abundant OPAHs were 9OFLN and (9,10)O_2ANT. OPAH patterns at Kladno, Mainz, and in the South Atlantic (own unpublished data) were very similar (significant on the P < 0.05, in most cases on the P < 0.01 level), whereas the patterns at Ostrava, winter and summer, were dissimilar. (9,10)O_2ANT represents about two-thirds of the quinones, 39−73% of Σ_6O_2PAHs in the gas and 63−83% in the particulate phase (campaign means). The consistently high fraction of (9,10)O_2ANT among OPAHs also at the rural background site, Košetice, and in the remote South Atlantic (unpublished own data) indicates a longer lifetime compared to other OPAHs, like (1,4)O_2NAP. (1,4)O_2NAP is very abundant close to primary sources and significantly less abundant in receptor areas.

3.3. Radicals. The EPR spectral characteristics of the $PM_{0.49}$ (Figure S8) and the g values of the particle-bound EPFR (2.00292 ± 0.00016) indicate that semiquinones are the major type of persistent free radicals in Košetice, Kladno and Ostrava $PM_{0.49}$,[82] similar to the ambient fine PM at other urban sites.[39,53,83−85] The observed abundance of EPFRs ranging from 0.8 to 4.0 pmol μg^{-1} (Table 2, Figure 1) are higher than the fine PM from urban sites in Germany (0.03−1.3 pmol μg^{-1}[53]) and PM from Saudi Arabia (0.02−0.1 pmol μg^{-1}, PM_{10}[86]), but similar to PM_{10} and $PM_{2.5}$ samples from urban sites in the USA (0.03−3.3 pmol μg^{-1}[87,88]). Furthermore, we found that EPFR concentration was correlated with the concentrations of water-soluble Fe (R = 0.89, Figure 1a) and quinones (Σ_6O_2PAH, R = 0.90, Figure 1b), respectively. These correlations are in line with previous findings and suggest that transition metals and quinones play an important role in the formation and/or stabilization of particulate EPFRs.[32,39,54,89−91] The concentrations of EPFRs (pmol m^{-3}) were similar to the O_2PAH concentrations at Košetice (winter) and Ostrava summer campaign, but were far higher by a factor of ≈5 and ≈40 during the urban winter campaigns, Ostrava and Kladno, respectively (Table 2). This suggests that particulate PAH and quinones near their

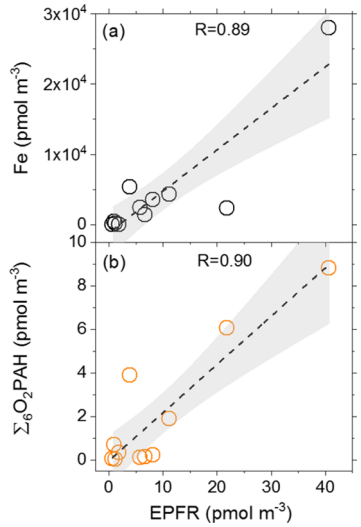

Figure 1. Concentrations and correlations of EPFRs with (a) water-soluble Fe and (b) total Σ_6O_2PAH in ambient PM. The shading areas represent 95% confidence bands.

combustion sources (in particular coal burning for domestic heating and industry use) are a stronger radical source than aged aerosol in the background and road traffic aerosol. Previous studies indicated that radical yield in particles, especially the •OH yield, is closely correlated with metal ions, metal−quinone interactions, and, upon inhalation and deposition into the LLF, on the interactions of metal ions and quinones with antioxidants.[54,92,93]

Based on the EPR measurement of particle sample extracts containing a spin-trapping agent 5-*tert*-butoxycarbonyl-5-methyl-1-pyrroline-*N*-oxide (BMPO[94]), we found that the $PM_{0.49}$ size fraction had a radical formation potential of 1.0−2.5 pmol m^{-3} (Figure S9b). This is comparable to the radical formation potential by $PM_{2.5}$ at an urban site in Germany, Mainz, but up to 1 order of magnitude lower than in megacities of China.[95] Such a finding is also in line with the previous finding that quinones and their derivatives could initiate redox-cycling reactions to generate reactive species including radicals.[9,96] Previous studies indicated that radical yield, especially the •OH yield, is closely correlated with metal ions, metal−quinone interactions, as well as the redox chemistry mediated by antioxidants.[54,92,93] Thus, it is important to assess the bioaccessibility of transition metals and aromatic compounds under physiological conditions.

3.4. Bioaccessibility. PM_1 samples, particles in the size range 3−10 μm (i.e., PM_{10}−PM_3) and PM_{10} samples of three campaigns were pooled such as to represent the entire sampling periods. LLFs used were ALF for the (PM_{10}−PM_3)

https://dx.doi.org/10.1021/acs.est.9b06820
Environ. Sci. Technol. 2020, 54, 2615−2625

and PM_{10} samples (Tables S4b and S5, Figure 2a) and both ALF and SELF for the PM_1 samples (Tables S4b and S5,

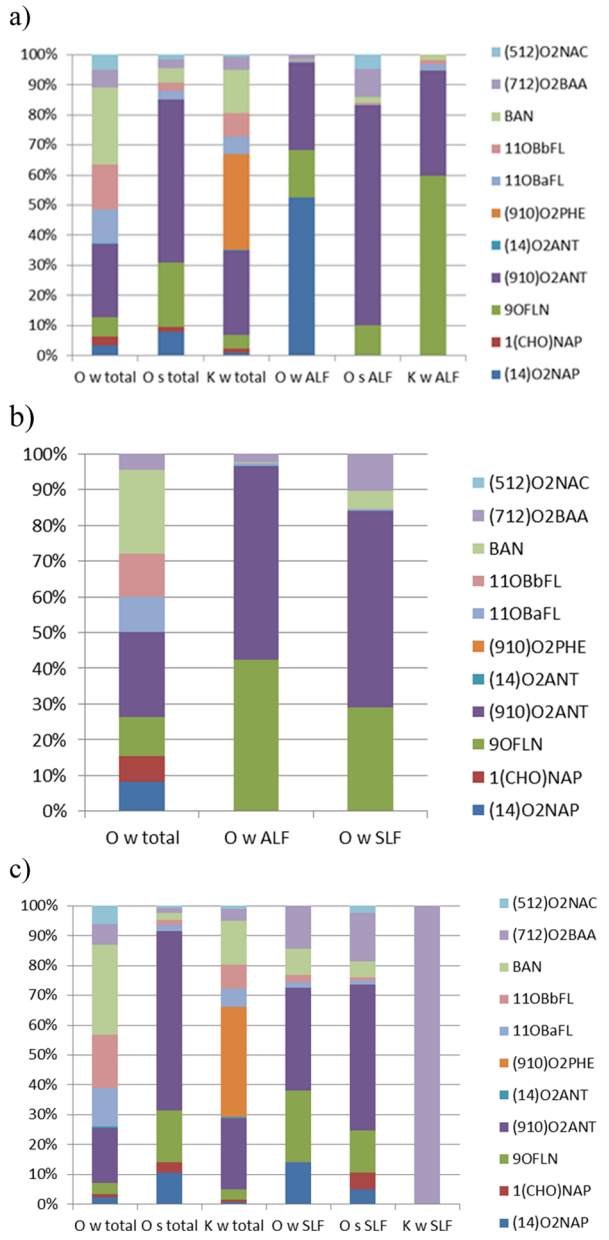

Figure 2. Particulate phase substance patterns of Σ_{10}OPAHs in the total (DCM extract) and bioaccessible fractions of (a,b) PM_{10} and (c) PM_1. The simulated epithelial lung lining fluids (LLFs) used were artificial lysosomal fluid (ALF, pH 4.5) and SELF (pH 7.4). O = Ostrava, K = Košetice, w = winter, s = summer.

Figure 2c) of the Košetice and both Ostrava campaigns. In addition, SELF was used to leach the PM_{10} sample of the Ostrava winter campaign (Figure 2b).

For NPAHs, bioaccessibility could not be confirmed. In PM_{10}, <0.01 and <0.1% was found as an upper limit in ALF and SELF, respectively (Ostrava winter, Table 3), where total NPAH was well above the LOQ (Table 1). Much higher upper limits of leached fractions are derived as a consequence of total NPAH concentrations being close to or below the LOQ (Table S3a). In summary, it is found that from filter samples containing NPAH well above the LOQ (i.e., PM_1 and PM_{10} collected at Ostrava), NPAHs bioaccessibility was <2% for both seasons and both LLFs used (Table 3).

OPAHs are more bioaccessible, that is, a few percent for the substance class as a whole, Σ_{10}OPAH, using both LLFs (Table 3). Highest f_{bio_p} is found for the two three-ring OPAHs, that is, up to 86 and 4.4% is found for 9OFLN using ALF and SELF (for different size fractions), respectively, and up to 18 and 3.4%, respectively, for (9,10)O_2ANT (Table S5).Four- to five-ring OPAHs' bioaccessibility corresponds to mostly $f_{bio\_p} \leq$ 1%, but for (7,12)O_2BAA and (5,12)O_2NAC can reach 2.4 and 3.3%, respectively (Table S5). Using ALF, f_{bio_p} of OPAHs associated with PM_1 and PM_{10} does not differ significantly (Tables 3a and S5). This is consistent with the perception that an electrolyte (ALF) dissolves polar substances (OPAHs) regardless the hydrophobicity of the matrix. However, in the Ostrava winter campaign, OPAHs associated with coarse mode particles (PM_{10}–PM_3) were found much more bioaccessible than those associated with PM_1 (42 vs 3.4%; Table 3a). Using SELF, f_{bio_p} of OPAHs associated with PM_{10} was found higher than of OPAHs associated with PM_1, except for (7,12)O_2BAA (Tables 3b and S5). More OPAHs were leached by SELF than by ALF in PM_1 samples of Ostrava summer, but the other way round in PM_1 samples collected in Košetice and Ostrava winter (Table S5). These trends are likely determined by aerosol matrices of various lipophilicities. For two cases of very low absolute concentrations (0.0027 ng m^{-3} 1(CHO)NAP and 0.0025 ng m^{-3} (1,4)O_2NAP), ALF leached masses seemingly exceeded total masses by up to 32 and 10%, respectively (Table S5). This we attribute to the larger uncertainties close to LOQ, when blank values varied considerably. The bioaccessible fraction's mass size distribution using ALF was shifted to larger particles for OPAHs in Ostrava in summer (Table S4). Other shifts of MSDs, from total dissolved to leached, that is, OPAHs in Ostrava and in Košetice in winter were less significant (Table S4).

In summary, inhalation bioaccessibility of polyaromatic pollutants in PM as defined by leaching filter samples in simulated lung fluid, is found low for both an acidic aqueous electrolyte (pH 4.5, ALF) and a neutral aqueous electrolyte with lipids, proteins, and antioxidants (pH 7.4, SELF), with few exceptions (9OFLN, (9,10)O_2ANT). However, this quantification of bioaccessibility does not fully represent the real conditions in the lung. As stated in the introduction, ultrafine particles may even penetrate through the membrane and thus deliver pollutants without dissolution in the lung fluid. Furthermore, the approach is not accounting for the possible release of additional pollutants from the PM to the lung fluid in the context of re-relaxation to equilibrium after the pollutant has reacted in the lung fluid. This could be a significant process as the residence time of PM for the tracheobronchial pathway is around 24 h and for the alveolar region between 1 week and thousands of days.[97]

Our findings emphasize the significance of the aerosol gas-phase for the targeted substance classes: NPAHs were gaseous in summer (for Σ_{18}NPAH, θ = 0.03 in summer but ranges 0.76–0.96 across winter campaigns) and OPAHs to a significant mass fraction also in winter (for Σ_{10}OPAH, θ ranges 0.38–0.88 across winter campaigns; Table S3). This is important for the assessment of the atmospheric fate, as it suggests a high long-range transport potential of these pollutants. The MSDs leaning toward the submicron size range highlight the significance of NPAHs' and OPAHs' inhalation exposure of also the deep lung, which is consistent

https://dx.doi.org/10.1021/acs.est.9b06820
Environ. Sci. Technol. 2020, 54, 2615–2625

Table 3. Concentrations (pg m^{-3}) of Bioaccessible Particulate Mass (in Brackets Bioaccessible Fraction f_{bio_p}) of OPAH and NPAH in Various PM Size Fractions[a,b]

a				
		rural background	urban	
ALF		Košetice winter	Ostrava winter	Ostrava summer
Σ_{10}OPAH	PM_{10}	20 (6.6%)	298 (4.0%)	12 (1.2%)
	PM_{10}–PM_3	0.06 (0.9%)	32 (42%)	1.3 (3.7%)
	PM_1	20 (7.5%)	204 (3.4%)	8.3 (9.2%)
Σ_{18}NPAH	PM_{10}	<2.5 (<4.4%)	<0.15 (<0.01%)	<0.10 (<2.3%)
	PM_{10}–PM_3	<2.5 (<245%)	<0.06 (<1.0%)	<0.10 (<27%)
	PM_1	<1.0 (<32%)	<0.15 (<0.01%)	<0.10 (<0.25%)
b				
		rural background	urban	
SELF		Košetice winter	Ostrava winter	Ostrava summer
Σ_{10}OPAH	PM_{10}	33 (8.2%)	141 (1.8%)	n.d.
	PM_1	12 (4.6%)	69 (1.2%)	19 (2.1%)
Σ_{18}NPAH	PM_{10}	<1.0 (<8.3%)	<1.2 (<0.1%)	n.d.
	PM_1	<0.35 (<3.3%)	<0.20 (<0.02%)	<0.12 (<1.7%)

[a]The simulated epithelial lung lining fluids (LLFs) used were (a) ALF (pH 4.5) and (b) SELF (pH 7.4). [b]n.d. = no data.

with other aromatic combustion by-products like the parent PAHs,[79] PCDD/Fs,[98] and nitrated monoaromatics.[70]

Particulate PAH and quinones are strong radical sources, in particular close to the combustion sources. The radical yield, especially the •OH yield depends on metal ions, and in the LLF, on antioxidants' availability.[54,93] Thus, it is important to assess the bioaccessibility of transition metals and aromatic compounds under physiological conditions. (9,10)O_2ANT which represented two-thirds of the quinones targeted has been neglected in ROS production estimates.[92,96]

Based on our working assumption that dissolution in LLF is a prerequisite for inhalation exposure to pollutants associated with PM, we conclude that the bioaccessibility is low for the particulate NPAHs (f_{bio_p} up to 1%). Because of concentrations <LOQ this was not verified for the carcinogenic N_2PYRs. Nevertheless, this is important for the related health risk assessment and for choice of threshold values for human exposure to these substances in ambient air. Bioaccessibility is relatively high, however, for three-ring OPAHs in PM, which is likely influenced by their polarity. This study warrants further efforts to study the inhalation exposure to the gaseous mass fraction of semivolatile organics, in particular PAHs and their derivatives, in ambient air.

■ ASSOCIATED CONTENT

Supporting Information

The Supporting Information is available free of charge at https://pubs.acs.org/doi/10.1021/acs.est.9b06820.

Sites, chemical analysis, observed concentrations, substance patterns and mass size distributions, and bioaccessible fractions (PDF)

■ AUTHOR INFORMATION

Corresponding Author

Gerhard Lammel − *Research Centre for Toxic Compounds in the Environment, Masaryk University, Brno 601 77, Czech Republic; Multiphase Chemistry Department, Max Planck Institute for Chemistry, Mainz 55128, Germany;* orcid.org/0000-0003-2313-0628; Phone: 420 54949 4106; Email: gerhard.lammel@recetox.muni.cz

Authors

Zoran Kitanovski − *Multiphase Chemistry Department, Max Planck Institute for Chemistry, Mainz 55128, Germany*

Petr Kukučka − *Research Centre for Toxic Compounds in the Environment, Masaryk University, Brno 601 77, Czech Republic*

Jiří Novák − *Research Centre for Toxic Compounds in the Environment, Masaryk University, Brno 601 77, Czech Republic*

Andrea M. Arangio − *Multiphase Chemistry Department, Max Planck Institute for Chemistry, Mainz 55128, Germany*

Garry P. Codling − *Research Centre for Toxic Compounds in the Environment, Masaryk University, Brno 601 77, Czech Republic*

Alexander Filippi − *Multiphase Chemistry Department, Max Planck Institute for Chemistry, Mainz 55128, Germany*

Jan Hovorka − *Faculty of Science, Institute for Environmental Studies, Charles University, Prague 116 36, Czech Republic*

Jan Kuta − *Research Centre for Toxic Compounds in the Environment, Masaryk University, Brno 601 77, Czech Republic*

Cecilia Leoni − *Faculty of Science, Institute for Environmental Studies, Charles University, Prague 116 36, Czech Republic*

Petra Příbylová − *Research Centre for Toxic Compounds in the Environment, Masaryk University, Brno 601 77, Czech Republic*

Roman Prokeš − *Research Centre for Toxic Compounds in the Environment, Masaryk University, Brno 601 77, Czech Republic*

Ondřej Sáňka − *Research Centre for Toxic Compounds in the Environment, Masaryk University, Brno 601 77, Czech Republic*

Pourya Shahpoury − *Multiphase Chemistry Department, Max Planck Institute for Chemistry, Mainz 55128, Germany; Air Quality Processes Research Section, Environment and Climate Change Canada, Toronto 12843, Canada*

Haijie Tong − *Multiphase Chemistry Department, Max Planck Institute for Chemistry, Mainz 55128, Germany;* orcid.org/0000-0001-9887-7836

Marco Wietzoreck − *Multiphase Chemistry Department, Max Planck Institute for Chemistry, Mainz 55128, Germany*

https://dx.doi.org/10.1021/acs.est.9b06820
Environ. Sci. Technol. 2020, 54, 2615−2625

Complete contact information is available at: https://pubs.acs.org/10.1021/acs.est.9b06820

Author Contributions

G.L. conceived the study. J.H., C.L., G.L., R.P., and O.S. conducted the air sampling and field measurements. Z.K., P.S., and M.W. developed and applied the analytical methods for bioaccessibility measurements. G.P.C., J.K., P.K., and P.P. did the chemical and A.M.A. and A.F. did the ESR analysis of the samples. A.M.A., G.L., J.N. and H.T. did the data analysis. G.L. discussed the results and wrote the paper with input from all the co-authors.

Notes

The authors declare no competing financial interest.

■ ACKNOWLEDGMENTS

We thank Libor Černikovský, Blanka Krejci, Jana Schovánková, Pavel Smolík, and Milan Váňa (Czech Hydrometeorological Institute) for access to stations and meteorological and trace gas data, Rostislav Červenka (MU) for carbon fractions data and Klára Hilscherová (MU) for discussion. This research was supported by the Czech Science Foundation (503/16/11537S, 503/12/G147), by the ACTRIS-CZ (LM2018122, CZ.02.1.01/0.0/0.0/16_013/0001315) and RECETOX (LM2018121) Research Infrastructures funded by the Ministry of Education, Youth and Sports of the Czech Republic, by the European Commission H2020 (CETOCOEN EXCELLENCE Teaming 2, #857560) and by the Max Planck Society.

■ REFERENCES

(1) Lewtas, J. Complex mixtures of air pollutants: characterizing the cancer risk of polycyclic organic matter. *Environ. Health Persp.* **1993**, *100*, 211−218.
(2) Jones, A. P. Indoor air quality and health. *Atmos. Environ.* **1999**, *33*, 4535−4564.
(3) ECHA, European Chemicals Agency. Candidate list of substances of very high concern for authorisation published in accordance with Article 59(10) of the REACH regulation. 2019, https://echa.europa.eu/candidate-list-table?_cldee=bGFtbWVsQHJlY2V0b3gubXVuaS5jeg%3d%3dandrecipientid=lead-aeed4f21fc79e81181000050569552b31-eb7ae0105c8d48d4a93b0dc66666ade8andesid=3472782f-9da7-e911-810f-005056b9310e (last time accessed July 15, 2019).
(4) IARC, International Agency for Research on Cancer. Some non-heterocyclic polycyclic aromatic hydrocarbons and some related exposures. *IARC Monogr Eval Carcinog Risks Hum.* **2010**, *92*, 1−853.
(5) WHO, World Health Organization. *Health Risks of Persistent Organic Pollutants from Long-Range Transboundary Air Pollution*; WHO Regional Office for Europe: Copenhagen, 2003.
(6) Ghio, A. J.; Soukup, J. M.; Madden, M. C. The toxicology of air pollution predicts its epidemiology. *Inhal. Toxicol.* **2018**, *30*, 327−334.
(7) Idowu, O.; Semple, K. T.; Ramadass, K.; O'Connor, W.; Hansbro, P.; Thavamani, P. Beyond the obvious: Environmental health implications of polar polycyclic aromatic hydrocarbons. *Environ. Intl.* **2019**, *123*, 543−557.
(8) Misaki, K.; Takamura-Enya, T.; Ogawa, H.; Takamori, K.; Yanagida, M. Tumour-promoting activity of polycyclic aromatic hydrocarbons and their oxygenated or nitrated derivatives. *Mutagenesis* **2016**, *31*, 205−213.
(9) Bolton, J. L.; Trush, M. A.; Penning, T. M.; Dryhurst, G.; Monks, T. J. Role of quinones in toxicology†. *Chem. Res. Toxicol.* **2000**, *13*, 135−160.
(10) Cassee, F. R.; Héroux, M.-E.; Gerlofs-Nijland, M. E.; Kelly, F. J. Particulate matter beyond mass: recent health evidence on the role of fractions, chemical constituents and sources of emission. *Inhal. Toxicol.* **2013**, *25*, 802−812.
(11) Sies, H.; Berndt, C.; Jones, D. P. Oxidative stress. *Ann. Rev. Biochem.* **2017**, *86*, 715−748.
(12) Siak, J.; Chan, T. L.; Gibson, T. L.; Wolff, G. T. Contribution to bacterial mutagenicity from nitro-PAH compounds in ambient aerosols. *Atmos. Environ.* **1985**, *19*, 369−376.
(13) *Nitroarenes − Occurrence, Metabolism, and Biological Impact*; Howard, P. C., Hecht, S. S., Beland, F. A., Eds.; Environmental Science Research 40; Plenum: New York, 1990.
(14) Yaffe, D.; Cohen, Y.; Arey, J.; Grosovsky, A. J. Multimedia Analysis of PAHs and Nitro-PAH Daughter Products in the Los Angeles Basin. *Risk Anal.* **2001**, *21*, 275−294.
(15) IARC, International Agency for Research on Cancer. Diesel and gasoline engine exhausts and some nitroarenes, *IARC Monographs on the Evaluation of Carcinogenic Risks to Humans*; IARC: Lyon, 2013; Vol. *105*, p 714.
(16) Geier, M. C.; Chlebowski, A. C.; Truong, L.; Massey Simonich, S. L.; Anderson, K. A.; Anderson, K. A.; Tanguay, R. L. Comparative developmental toxicity of a comprehensive suite of polycyclic aromatic hydrocarbons. *Arch. Toxicol.* **2018**, *92*, 571−586.
(17) Walgraeve, C.; Demeestere, K.; Dewulf, J.; Zimmermann, R.; van Langenhove, H. Oxygenated polycyclic aromatic hydrocarbons in atmospheric particulate matter: Molecular characterization and occurrence. *Atmos. Environ.* **2010**, *44*, 1831−1846.
(18) Lammel, G. Polycyclic aromatic compounds in the atmosphere - a review identifying research needs. *Polycyclic Aromat. Compd.* **2015**, *35*, 316−329.
(19) Bandowe, B. A. M.; Meusel, H. Nitrated polycyclic aromatic hydrocarbons (nitro-PAHs) in the environment - A review. *Sci. Total Environ.* **2017**, *581−582*, 237−257.
(20) Finlayson-Pitts, B. J.; Pitts, J. N. *Chemistry of the Upper and Lower Atmosphere: Theory, Experiments, Application*; Academic Press: San Diego, USA, 2002.
(21) Keyte, I. J.; Harrison, R. M.; Lammel, G. Chemical reactivity and long-range transport potential of polycyclic aromatic hydrocarbons - a review. *Chem. Soc. Rev.* **2013**, *42*, 9333−9391.
(22) Li, W.; Wang, C.; Shen, H.; Su, S.; Shen, G.; Huang, Y.; Zhang, Y.; Chen, Y.; Chen, H.; Lin, N.; Zhuo, S.; Zhong, Q.; Wang, X.; Liu, J.; Li, B.; Liu, W.; Tao, S. Concentrations and origins of nitro-polycyclic aromatic hydrocarbons and oxy-polycyclic aromatic hydrocarbons in ambient air in urban and rural areas in northern China. *Envion. Pollut.* **2015**, *197*, 156−164.
(23) Lin, Y.; Ma, Y.; Qiu, X.; Li, R.; Fang, Y.; Wang, J.; Zhu, Y.; Hu, D. Sources, transformation, and health implications of PAHs and their nitrated, hydroxylated, and oxygenated derivatives in $PM_{2.5}$ in Beijing. *J. Geophys. Res.* **2015**, *120*, 7219−7228.
(24) Tomaz, S.; Shahpoury, P.; Jaffrezo, J.-L.; Lammel, G.; Perraudin, E.; Villenave, E.; Albinet, A. One-year study of polycyclic aromatic compounds at an urban site in Grenoble (France): Seasonal variations, gas/particle partitioning and cancer risk estimation. *Sci. Total Environ.* **2016**, *565*, 1071−1083.
(25) Zhang, J.; Yang, L.; Mellouki, A.; Chen, J.; Chen, X.; Gao, Y.; Jiang, P.; Li, Y.; Yu, H.; Wang, W. Atmospheric PAHs, NPAHs, and OPAHs at an urban, mountainous, and marine sites in Northern China: Molecular composition, sources, and ageing. *Atmos. Environ.* **2018**, *173*, 256−264.
(26) Hayakawa, K.; Tang, N.; Nagato, E. G.; Toriba, A.; Sakai, S.; Kano, F.; Goto, S.; Endo, O.; Arashidani, K.-i.; Kakimoto, H. Long term trends in atmospheric concentrations of polycyclic aromatic hydrocarbons and nitropolycyclic aromatic hydrocarbons: A study of Japanese cities from 1997 to 2014. *Environ. Pollut.* **2018**, *233*, 474−482.
(27) Ciccioli, P.; Cecinato, A.; Brancaleoni, E.; Frattoni, M.; Zacchei, P.; Miguel, A. H.; de Castro Vasconcellos, P. Formation and transport of 2-nitrofluoranthene and 2-nitropyrene of photochemical origin in the troposphere. *J. Geophys. Res.* **1996**, *101*, 19567−19581.
(28) Tsapakis, M.; Stephanou, E. G. Diurnal Cycle of PAHs, Nitro-PAHs, and oxy-PAHs in a High Oxidation Capacity Marine Background Atmosphere. *Environ. Sci. Technol.* **2007**, *41*, 8011−8017.

(29) Lafontaine, S.; Schrlau, J.; Butler, J.; Jia, Y.; Harper, B.; Harris, S.; Bramer, L. M.; Waters, K. M.; Harding, A.; Simonich, S. L. M. Relative influence of trans-pacific and regional atmospheric transport of PAHs in the pacific northwest, U.S. *Environ. Sci. Technol.* **2015**, *49*, 13807−13816.
(30) Harrison, R. M.; Alam, M. S.; Dang, J.; Ismail, I. M.; Basahi, J.; Alghamdi, M. A.; Hassan, I. A.; Khoder, M. Relationship of polycyclic aromatic hydrocarbons with oxy(quinone) and nitro derivatives during air mass transport. *Sci. Total Environ.* **2016**, *572*, 1175−1183.
(31) Lammel, G.; Mulder, M. D.; Shahpoury, P.; Kukučka, P.; Lišková, H.; Přibylová, P.; Prokeš, R.; Wotawa, G. Nitro-polycyclic aromatic hydrocarbons - gas-particle partitioning, mass size distribution, and formation along transport in marine and continental background air. *Atmos. Chem. Phys.* **2017**, *17*, 6257−6270.
(32) Borrowman, C. K.; Zhou, S.; Burrow, T. E.; Abbatt, J. P. D. Formation of environmentally persistent free radicals from the heterogeneous reaction of ozone and polycyclic aromatic compounds. *Phys. Chem. Chem. Phys.* **2016**, *18*, 205−212.
(33) Monks, T. J.; Hanzlik, R. P.; Cohen, G. M.; Ross, D.; Graham, D. G. Quinone chemistry and toxicity. *Toxicol. Appl. Pharmacol.* **1992**, *112*, 2−16.
(34) Andersson, H.; Piras, E.; Demma, J.; Hellman, B.; Brittebo, E. Low levels of the air pollutant 1-nitropyrene induce DNA damage, increased levels of reactive oxygen species and endoplasmic reticulum stress in human endothelial cells. *Toxicology* **2009**, *262*, 57−64.
(35) Park, E.-J.; Park, K. Induction of pro-inflammatory signals by 1-nitropyrene in cultured BEAS-2B cells. *Toxicol. Lett.* **2009**, *184*, 126−133.
(36) Øvrevik, J.; Arlt, V. M.; Øya, E.; Nagy, E.; Mollerup, S.; Phillips, D. H.; Låg, M.; Holme, J. A. Differential effects of nitro-PAHs and amino-PAHs on cytokine and chemokine responses in human bronchial epithelial BEAS-2B cells. *Toxicol. Appl. Pharmacol.* **2010**, *242*, 270−280.
(37) Tuet, W. Y.; Liu, F.; de Oliveira Alves, N.; Fok, S.; Artaxo, P.; Vasconcellos, P.; Champion, J. A.; Ng, N. L. Chemical oxidative potential and cellular oxidative stress from open biomass burning aerosol. *Environ. Sci. Technol. Lett.* **2019**, *6*, 126−132.
(38) Shiraiwa, M.; Ueda, K.; Pozzer, A.; Lammel, G.; Kampf, C. J.; Fushimi, A.; Enami, S.; Arangio, A. M.; Fröhlich-Nowoisky, J.; Fujitani, Y.; Furuyama, A.; Lakey, P. S. J.; Lelieveld, J.; Lucas, K.; Morino, Y.; Pöschl, U.; Takahama, S.; Takami, A.; Tong, H.; Weber, B.; Yoshino, A.; Sato, K. Aerosol health effects from molecular to global scales. *Environ. Sci. Technol.* **2017**, *51*, 13545−13567.
(39) Vejerano, E. P.; Rao, G.; Khachatryan, L.; Cormier, S. A.; Lomnicki, S. Environmentally persistent free radicals: Insights on a new class of pollutants. *Environ. Sci. Technol.* **2018**, *52*, 2468−2481.
(40) Oberdörster, G.; Sharp, Z.; Atudorei, V.; Elder, A.; Gelein, R.; Kreyling, W.; Cox, C. Translocation of inhaled ultrafine particles to the brain. *Inhal. Toxicol.* **2004**, *16*, 437−445.
(41) Li, X.-Y.; Hao, L.; Liu, Y.-H.; Chen, C.-Y.; Pai, V. J.; Kang, J. X. Protection against fine particle-induced pulmonary and systemic inflammation by omega-3 polyunsaturated fatty acids. *Biochim. Biophys. Acta* **2017**, *1861*, 577−584.
(42) Wiseman, C. L. S.; Zereini, F. Characterizing metal(loid) solubility in airborne PM_{10}, $PM_{2.5}$ and PM_1 in Frankfurt, Germany using simulated lung fluids. *Atmos. Environ.* **2014**, *89*, 282−289.
(43) Polezer, G.; Oliveira, A.; Potgieter-Vermaak, S. P.; Godoi, A. F. L.; de Souza, R. A. F.; Yamamoto, C. I.; Andreoli, R. V.; Medeiros, A. S.; Machado, C. M. D.; dos Santos, E. O.; de André, P. A.; Pauliquevis, T.; Saldiva, P. H. N.; Martin, S. T.; Godoi, R. H. M. The influence that different urban development models has on $PM_{2.5}$ elemental and bioaccessible Profiles. *Sci. Rep.* **2019**, *9*, 14846.
(44) Wei, W.; Bonvallot, N.; Gustafsson, Å.; Raffy, G.; Glorennec, P.; Krais, A.; Ramalho, O.; le Bot, B.; Mandin, C. Bioaccessibility and bioavailability of environmental semi-volatile organic compounds via inhalation: A review of methods and models. *Environ. Int.* **2018**, *113*, 202−213.
(45) Nováková, Z.; Novák, J.; Kitanovski, Z.; Kukučka, P.; Přibylová, P.; Prokeš, R.; Smutná, M.; Wietzoreck, M.; Lammel, G.; Hilscherová, K. Toxic potentials of particulate and gaseous air pollution and the role of PAHs and their derivatives. *Environ. Int.* **2019**, submitted.
(46) Pokorná, P.; Hovorka, J.; Klán, M.; Hopke, P. K. Source apportionment of size resolved particulate matter at a European air pollution hot spot. *Sci. Total Environ.* **2015**, *502*, 172−183.
(47) Pokorná, P.; Hovorka, J.; Hopke, P. K. Elemental composition and source identification of very fine aerosol particles in a European air pollution hot-spot. *Air Pollut. Res.* **2016**, *7*, 671−679.
(48) Kozáková, J.; Pokorná, P.; Vodička, P.; Ondráčková, L.; Ondráček, J.; Křůmal, K.; Mikuška, P.; Hovorka, J.; Moravec, P.; Schwarz, J. The influence of local emissions and regional air pollution transport on a European air pollution hot spot. *Environ. Sci. Pollut. Res.* **2019**, *26*, 1675−1692.
(49) Líbalová, H.; Uhlířová, K.; Kléma, J.; Machala, M.; Šrám, R. J.; Ciganek, M.; Topinka, J. Global gene expression changes in human embryonic lung fibroblasts induced by organic extracts from respirable air particles. *Part. Fibre Toxicol.* **2012**, *9*, 1−16.
(50) Šram, R. J.; Dostal, M.; Libalová, H.; Rossner, P.; Rossnerová, A.; Svečová, V.; Topinka, T.; Bartonová, A. *The European Hot Spot of B[a]P and $PM_{2.5}$ Exposure—The Ostrava region. Czech Republic: Health Research Results*; ISRN Public Health, 2013; p 416071.
(51) Topinka, J.; Rossner, P.; Milcová, A.; Schmuczerová, J.; Pěnčíková, K.; Rossnerová, A.; Ambrož, A.; Štolcpartová, J.; Bendl, J.; Hovorka, J.; Machala, M. Day-to-day variability of toxic events induced by organic compounds bound to size segregated atmospheric aerosol. *Environ. Pollut.* **2015**, *202*, 135−145.
(52) Leoni, C.; Hovorka, J.; Dočekalová, V.; Cajthaml, T.; Marvanová, S. Source impact determination using airborne and ground measurements of industrial plumes. *Environ. Sci. Technol.* **2016**, *50*, 9881−9888.
(53) Arangio, A. M.; Tong, H.; Socorro, J.; Pöschl, U.; Shiraiwa, M. Quantification of environmentally persistent free radicals and reactive oxygen species in atmospheric aerosol particles. *Atmos. Chem. Phys.* **2016**, *16*, 13105−13119.
(54) Tong, H.; Lakey, P. S. J.; Arangio, A. M.; Socorro, J.; Shen, F.; Lucas, K.; William, H.; Brune, W. H.; Pöschl, U.; Shiraiwa, M. Reactive oxygen species formed by secondary organic aerosols in water and surrogate lung fluid. *Environ. Sci. Technol.* **2018**, *52*, 11642−11651.
(55) Colombo, C.; Monhemius, A. J.; Plant, J. A. Platinum, palladium and rhodium release from vehicle exhaust catalysts and road dust exposed to simulated lung fluids. *Ecotox. Environ. Safety* **2008**, *71*, 722−730.
(56) Boisa, N.; Elom, N.; Dean, J. R.; Deary, M. E.; Bird, G.; Entwistle, J. A. Development and application of an inhalation bioaccessibility method (IBM) for lead in the PM_{10} size fraction of soil. *Environ. Int.* **2014**, *70*, 132−142.
(57) Holoubek, I.; Klánová, J.; Jarkovský, J.; Kohoutek, J. Trends in background levels of persistent organic pollutants at Kosetice observatory, Czech Republic. : Part I. Ambient air and wet deposition 1996-2005. *J. Environ. Mon.* **2007**, *9*, 557−563.
(58) Lammel, G.; Novák, J.; Landlová, L.; Dvorská, A.; Klánová, J.; Čupr, P.; Kohoutek, J.; Reimer, E.; Škrdlíková, L. Sources and distributions of polycyclic aromatic hydrocarbons and toxicity of polluted atmosphere aerosols. In *Urban Airborne Particulate Matter: Origins, Chemistry, Fate and Health Impacts*; Zereini, F., Wiseman, C. L. S., Eds.; Springer: Berlin, 2010; pp 39−62.
(59) Dvorská, A.; Komprdová, K.; Lammel, G.; Klánová, J.; Plachá, H. Polycyclic aromatic hydrocarbons in background air in central Europe − seasonal levels and limitations for source apportionment. *Atmos. Environ.* **2012**, *46*, 147−154.
(60) CHMI. Air Pollution in the Czech Republic 2013. *Graphic Yearbook*; Czech Hydrometeorological Institute: Prague, 2014, http://portal.chmi.cz/files/portal/docs/uoco/isko/grafroc/13groc/gr13e/Obsah_GB.html (last time accessed November 10, 2019).
(61) Vossler, T.; Černikovsky, L.; Novák, J.; Plachá, H.; Krejci, B.; Nikolová, I.; Chalupníčková, E.; Williams, R. An investigation of local and regional sources of fine particulate matter in Ostrava, the Czech Republic. *Atmos. Pollut. Res.* **2015**, *6*, 454−463.

https://dx.doi.org/10.1021/acs.est.9b06820
Environ. Sci. Technol. 2020, 54, 2615−2625

(62) Degrendele, C.; Fiedler, H.; Kočan, A.; Kukučka, P.; Přibylová, P.; Prokeš, R.; Klánová, J.; Lammel, G. Multiyear levels of PCDD/Fs, dl-PCBs and PAHs in background air in central Europe and implications for deposition. *Chemosphere* **2020**, *240*, 124852.
(63) Srivastava, D.; Tomaz, S.; Favez, O.; Lanzafame, G. M.; Golly, B.; Besombes, J.-L.; Alleman, L. Y.; Jaffrezo, J.-L.; Jacob, V.; Perraudin, E.; Villenave, E.; Albinet, A. Speciation of organic fraction does matter for source apportionment. Part 1: A one-year campaign in Grenoble (France). *Sci Tot. Environ.* **2018**, *624*, 1598−1611.
(64) Lammel, G.; Brüggemann, E.; Gnauk, T.; Müller, K.; Neusüss, C.; Röhrl, A. A new method to study aerosol source contributions along the tracks of air parcels and its application to the near-ground level aerosol chemical composition in central Europe. *J. Aerosol Sci.* **2003**, *34*, 1−25.
(65) Shahpoury, P.; Lammel, G.; Albinet, A.; Sofuoğlu, A.; Dumanoğlu, Y.; Sofuoğlu, S. C.; Wagner, Z.; Ždimal, V. Evaluation of a conceptual model for gas-particle partitioning of polycyclic aromatic hydrocarbons using polyparameter linear free energy relationships. *Environ. Sci. Technol.* **2016**, *50*, 12312−12319.
(66) Shahpoury, P.; Kitanovski, Z.; Lammel, G. Snow scavenging and phase partitioning of nitrated and oxygenated aromatic hydrocarbons in polluted and remote environments in central Europe and the European Arctic. *Atmos. Chem. Phys.* **2018**, *18*, 13495−13510.
(67) Wang, W.; Simonich, S. L. M.; Wang, W.; Giri, B.; Zhao, J.; Xue, M.; Cao, J.; Lu, X.; Tao, S. Atmospheric polycyclic aromatic hydrocarbon concentrations and gas/particle partitioning at background, rural village and urban sites in the North China Plain. *Atmos. Res.* **2011**, *99*, 197−206.
(68) Verma, P. K.; Sah, D.; Kumari, K. M.; Lakhani, A. Atmospheric concentrations and gas-particle partitioning of polycyclic aromatic hydrocarbons (PAHs) and nitro-PAHs at Indo-Gangetic sites. *Environ. Sci. Proc. Imp.* **2017**, *19*, 1051−1060.
(69) CZSO. Energo 2015; Czech Statistical Office, 2015, https://www.czso.cz/csu/czso/o-setreni-energo-2015 (last time accessed July 1, 2019).
(70) Kitanovski, Z.; Shahpoury, P.; Samara, C.; Voliotis, A.; Lammel, G. Mass size distribution of nitrated and oxygenated aromatic compounds in ambient particulate matter from southern and central Europe − contribution to humic-like substances. *Atmos. Chem. Phys.* **2020**, *20* DOI: 10.5194/acp-2019-673.
(71) Huang, W.; Huang, B.; Bi, X.; Lin, Q.; Liu, M.; Ren, Z.; Zhang, G.; Wang, X.; Sheng, G.; Fu, J. Emission of PAHs, NPAHs and OPAHs from residential honeycomb coal briquette combustion. *Energy Fuels* **2014**, *28*, 636−642.
(72) Shen, G.; Chen, Y.; Du, W.; Lin, N.; Wang, X.; Cheng, H.; Liu, J.; Xue, C.; Liu, G.; Zeng, E. Y.; Xing, B.; Tao, S. Exposure and size distribution of nitrated and oxygenated polycyclic aromatic hydrocarbons among the population using different household fuels. *Environ. Pollut.* **2016**, *216*, 935−942.
(73) Leoni, C.; Pokorná, P.; Hovorka, J.; Masiol, M.; Topinka, J.; Zhao, Y.; Křůmal, K.; Cliff, S.; Mikuška, P.; Hopke, P. K. Source apportionment of aerosol particles at a European air pollution hot spot using particle number size distributions and chemical composition. *Environ. Pollut.* **2018**, *234*, 145−154.
(74) Mikuška, P.; Křůmal, K.; Večeřa, Z. Characterization of organic compounds in the $PM_{2.5}$ aerosols in winter in an industrial urban area. *Atmos. Environ.* **2015**, *105*, 97−108.
(75) *Odyssee − EC Project Odyssee-Mure, Energy Consumption Data Base*, 2016, http://www.indicators.odyssee-mure.eu/energy-efficiency-database.html.
(76) WHO, World Health Organization. *Global Urban Ambient Air Pollution Database* (Update 2016), 2016, http://www.who.int/phe/health_topics/outdoorair/databases/cities/en/ (accessed on August 12, 2019).
(77) Allen, J. O.; Dookeran, N. M.; Taghizadeh, K.; Lafleur, A. L.; Smith, K. A.; Sarofim, A. F. Measurement of oxygenated polycyclic aromatic hydrocarbons associated with a size-segregated urban aerosol. *Environ. Sci. Technol.* **1997**, *31*, 2064−2070.
(78) Albinet, A.; Leoz-Garziandia, E.; Budzinski, H.; Villenave, E.; Jaffrezo, J.-L. Nitrated and oxygenated derivatives of polycyclic aromatic hydrocarbons in the ambient air of two French alpine valleys Part 2: Particle size distribution. *Atmos. Environ.* **2008**, *42*, 55−64.
(79) Ringuet, J.; Leoz-Garziandia, E.; Budzinski, H.; Villenave, E.; Albinet, A. Particle size distribution of nitrated and oxygenated polycyclic aromatic hydrocarbons (NPAHs and OPAHs) on traffic and suburban sites of a European megacity: Paris (France). *Atmos. Chem. Phys.* **2012**, *12*, 8877−8887.
(80) di Filippo, P.; Riccardi, C.; Pomata, D.; Buiarelli, F. Concentrations of PAHs, and nitro- and methyl- derivatives associated with a size-segregated urban aerosol. *Atmos. Environ.* **2010**, *44*, 2742−2749.
(81) Mulder, M. D.; Dumanoglu, Y.; Efstathiou, C.; Kukučka, P.; Matejovičová, J.; Maurer, C.; Přibylová, P.; Prokeš, R.; Sofuoglu, A.; Sofuoglu, S. C.; Wilson, J.; Zetzsch, C.; Wotawa, G.; Lammel, G. Fast formation of nitro-PAHs in the marine atmosphere constrained in a regional-scale Lagrangian field experiment. *Environ. Sci. Technol.* **2019**, *53*, 8914−8924.
(82) Dellinger, B.; Lomnicki, S.; Khachatryan, L.; Maskos, Z.; Hall, R. W.; Adounkpe, J.; McFerrin, C.; Truong, H. Formation and stabilization of persistent free radicals. *Proc. Combust. Inst.* **2007**, *31*, 521−528.
(83) Gehling, W.; Dellinger, B. Environmentally persistent free radicals and their lifetimes in $PM_{2.5}$. *Environ. Sci. Technol.* **2013**, *47*, 8172−8178.
(84) Wang, P.; Pan, B.; Li, H.; Huang, Y.; Dong, X.; Ai, F.; Liu, L.; Wu, M.; Xing, B. The overlooked occurrence of environmentally persistent free radicals in an area with low-rank coal burning, Xuanwei, China. *Environ. Sci. Technol.* **2018**, *52*, 1054−1061.
(85) Chen, Q.; Sun, H.; Mu, Z.; Wang, Y.; Li, Y.; Zhang, L.; Wang, M.; Zhang, Z. Characteristics of environmentally persistent free radicals in $PM_{2.5}$: Concentrations, species and sources in Xi'an, Northwestern China. *Environ. Pollut.* **2019**, *247*, 18−26.
(86) Shaltout, A. A.; Boman, J.; Shehadeh, Z. F.; Al-Malawi, D.-a. R.; Hemeda, O. M.; Morsy, M. M. Spectroscopic investigation of $PM_{2.5}$ collected at industrial, residential and traffic sites in Taif, Saudi Arabia. *J. Aerosol Sci.* **2015**, *79*, 97−108.
(87) Squadrito, G. L.; Cueto, R.; Dellinger, B.; Pryor, W. A. Quinoid redox cycling as a mechanism for sustained free radical generation by inhaled airborne particulate matter. *Free Radical Biol. Med.* **2001**, *31*, 1132−1138.
(88) Gehling, W.; Khachatryan, L.; Dellinger, B. Hydroxyl radical generation from environmentally persistent free radicals (EPFRs) in $PM_{2.5}$. *Environ. Sci. Technol.* **2014**, *48*, 4266−4272.
(89) Jia, H.; Nulaji, G.; Gao, H.; Wang, F.; Zhu, Y.; Wang, C. Formation and Stabilization of Environmentally Persistent Free Radicals Induced by the Interaction of Anthracene with Fe(III)-Modified Clays. *Environ. Sci. Technol.* **2016**, *50*, 6310−6319.
(90) Jia, H.; Zhao, S.; Shi, Y.; Zhu, L.; Wang, C.; Sharma, V. K. Transformation of Polycyclic Aromatic Hydrocarbons and Formation of environmentally persistent free radicals on modified montmorillonite: the role of surface metal ions and polycyclic promatic hydrocarbon molecular properties. *Environ. Sci. Technol.* **2018**, *52*, 5725−5733.
(91) Zhao, S.; Gao, P.; Miao, D.; Wu, L.; Qian, Y.; Chen, S.; Sharma, V. K.; Jia, H. Formation and evolution of solvent-extracted and nonextractable environmentally persistent free radicals in fly ash of municipal solid waste incinerators. *Environ. Sci. Technol.* **2019**, *53*, 10120−10130.
(92) Charrier, J. G.; McFall, A. S.; Richards-Henderson, N. K.; Anastasio, C. Hydrogen peroxide formation in a surrogate lung fluid by transition metals and quinones present in particulate matter. *Environ. Sci. Technol.* **2014**, *48*, 7010−7017.
(93) Wei, J.; Yu, H.; Wang, Y.; Verma, V. Complexation of iron and copper in ambient particulate matter and its effect on the oxidative potential measured in a surrogate lung fluid. *Environ. Sci. Technol.* **2019**, *53*, 1661−1671.

https://dx.doi.org/10.1021/acs.est.9b06820
Environ. Sci. Technol. 2020, 54, 2615−2625

(94) Zhao, H.; Joseph, J.; Zhang, H.; Karoui, H.; Kalyanaraman, B. Synthesis and biochemical applications of a solid cyclic nitrone spin trap: a relatively superior trap for detecting superoxide anions and glutathiyl radicals. *Free Radical Biol. Med.* **2001**, *31*, 599−606.
(95) Tong, H.; Zhang, Y.; Filippi, A.; Wang, T.; Li, C.; Liu, F.; Leppla, D.; Kourtchev, I.; Wang, K.; Keskinen, H.-M.; Levula, J. T.; Arangio, A. M.; Shen, F.; Ditas, F.; Martin, S. T.; Artaxo, P.; Godoi, R. H. M.; Yamamoto, C. I.; de Souza, R. A. F.; Huang, R.-J.; Berkemeier, T.; Wang, Y.; Su, H.; Cheng, Y.; Pope, F. D.; Fu, P.; Yao, M.; Pöhlker, C.; Petäjä, T.; Kulmala, M.; Andreae, M. O.; Shiraiwa, M.; Pöschl, U.; Hoffmann, T.; Kalberer, M. Radical formation by fine particulate matter associated with highly oxygenated molecules. *Environ. Sci. Technol.* **2019**, *53*, 12506−12518.
(96) Lakey, P. S. J.; Berkemeier, T.; Tong, H.; Arangio, A. M.; Lucas, K.; Pöschl, U.; Shiraiwa, M. Chemical exposure-response relationship between air pollutants and reactive oxygen species in the human respiratory tract. *Sci. Rep.* **2016**, *6*, 32916.
(97) Julien, C.; Esperanza, P.; Bruno, M.; Alleman, L. Y. Development of an in vitro method to estimate lung bioaccessibility of metals from atmospheric particles. *J. Environ. Monit.* **2011**, *13*, 621−630.
(98) Zhang, X.; Zheng, M.; Liu, G.; Zhu, Q.; Dong, S.; Zhang, H.; Wang, X.; Xiao, K.; Gao, L.; Liu, W. A comparison of the levels and particle size distribution of lower chlorinated dioxin/furans (mono- to tri-chlorinated homologues) with those of tetra- to octa-chlorinated homologues in atmospheric samples. *Chemosphere* **2016**, *151*, 55−58.

https://dx.doi.org/10.1021/acs.est.9b06820
Environ. Sci. Technol. 2020, 54, 2615−2625